Structural characteristics and tribological properties of Ti-Al-Cr-(Si)-C-N nanocomposite films coated on the SPK 1.2080 tool steel using PVD technique

M. Hassan Dadkhah Tehrani[1], A. Jafari Tadi [1*], Y. Yaghoubi Askarabad[2], M. Karimian[2], K. Amini[3] and M. Hossein Dadkhah Tehrani[1]

[1] *Malek-Ashtar University of Technology, P.O. Box 83145-115, Isfahan, IR Iran.*
[2] *Islamic Azad University, P.O. Box 81595-158, Isfahan, IR Iran.*
[3] *Department of Mechanical Engineering, Tiran Branch, Islamic Azad University, Isfahan, Iran*

ARTICLE INFO

Article history:

Received 17 June 2016
Accepted 28 December 2016
Available online 15 March 2017

Keywords:

Tool steel
Ti-Al-Cr-(Si)-C-N
Microstructure
Tribological behavior

ABSTRACT

In the present work, structural characteristics and tribological properties of Ti-Al-Cr-(Si)-C-N nanocomposite films coated on SPK 1.2080 tool steel by PVD technique have been investigated. The PVD coating process was carried out using Ti (Si) Al and CrAl cathodes at 150 A current, 40 V bias and $(Ar)_{0.1}(CH_4)_{0.45}(N_2)_{0.45}$ gas mixture for 50 min. Evaluations were conducted by OM, FESEM, AFM, XRD, nano and micro-indenters, and pin-on-disk tribometer. The uniform films with an about 2.5 μm thickness and 11.7 and 9.5 nm crystallite size values were respectively formed on the Ti-Al-Cr-C-N and Ti-Al-Cr-(Si)-C-N coated specimens. Surface hardness of the Ti-Al-Cr-C-N and Ti-Al-Cr-Si-C-N-coated samples was respectively obtained 8.7 and 10.8 GPa compared to 2.16 GPa for the un-coated substrate. Roughness (RMS), reduced modulus (E) and H/E ratio related to the Si-incorporated film were respectively determined 4.6 nm, 477 GPa and 0.081 while the mentioned values were 9.7 nm, 364 GPa and 0.075 for the Si-emptied film. Tribological properties were significantly enhanced by both films particularly by the Si-incorporated kind.

1-Introduction

Many studies have been recently performed on the coating of nanostructured multicomponent hard films by physical vapor deposition (PVD) ways. These methods have different applications for production of industrial instruments such as punch, lathe and rolling devices manufactured by hard films as Ti-N, Cr-N, Ti-Al-N and Ti-Al-Cr-N types [1] due to the improvement of properties such as higher hardness, good adhesion, better wear resistance and sufficient corrosion resistance [1,2]. Initially, the films were mostly coated in binary status such as the Ti-N types which, unfortunately, have a limited utilization under high-temperature environment beyond 500 °C and high-speed dry machining processes [2, 3].

Afterwards, ternary films such as the Ti–Al–N [3], Cr–Ti–N [4, 5] and Ti–Si–N [6] types were utilized and developed as the researches exhibited that their performance can be significantly better than the binary kinds particularly in mechanical, thermal and tribological fields. Also, temperature endurance may be raised up to 700 °C [7]. According to studies, multicomponent films composed of metallic and non-metallic components combine benefits of individual elements, resulting in films with better properties [8]. Therefore, the

* Corresponding author:
E-mail: *abdolrezajafari68@gmail.com*

addition of soft and hard elements into the ternary films (e.g. Ti–Al–N films) can significantly improve their properties [8]. Ti–Al–N-based multicomponent films such as Ti–Al–Si–N [9], Ti–Al–Cr–N [10] and Ti–Al–Y–N [11] have been recently investigated. For example, the Ti–Al–Si–N film has a better wear resistance than Ti–Al–N without any Si [12]. On other hand, quaternary films such as Al–Ti–Cr–N, Ti–Al–Si–N and Ti–Cr–Si–N kinds can induce a better performance than the ternary films [3]. Moreover, pentamerous and senary films have been recently utilized and showed a better performance than quaternary coatings [7, 13].

With consideration of further applications of multicomponent films, structural characteristics and tribological behavior of pentamerous and senary Ti-Al-Cr-(Si)-C-N films as new coatings have been investigated for the first time in the present work. The PVD coating process was performed on the disc-shaped SPK 1.2080 cold-work tool steel substrates. FESEM, XRD, AFM, nano-indenter and tribometer instruments were used to evaluate of the coated films, characteristics.

2- Material and experimental procedure

2-1- Material

The PVD processes were carried out on the SPK 1.2080 cold-work tool steel machined in the form of disc-shaped specimens with 50 mm diameter and 7 mm height and 0.06 μm surface roughness (Ra). Chemical composition of the SPK 1.2080 tool steel has been shown in Table 1. The as-received material was in solution treated and quenched status with an average hardness of 16 HRC was pre-treated for the coating process by hardening and tempering treatments; initially, heating using 10-4 mbar vacuum at 600, 800 and 980 °C temperatures for 30 min and afterwards quenching in oil solution and finally tempering at 120 and 220 °C temperatures for 2 h, resulting in 60 HRC as the substrate hardness. Vacuum conditions led to a clean surface without oxide compounds, and the tempering led to a hardened and toughened substrate [5] regarding the SPK1.2080 tool steel industrial requirements.

Table 1. Chemical composition of the SPK 1.2080 tool steel in this work.

Element	C	Cr	Mn	Si	P	S	Fe
Wt. %	2.1	11.0	0.3	0.3	0.01	0.009	balance

2-2- The PVD process

Physical vapor deposition was carried out using a semi-industrial unit under reactive cathodic arc conditions. In this unit, the required temperature for the deposition process was achieved by heating outside the machine using an external heater, and then by sputtering and coating reactions inside the machine. Prior to loading into the machine chamber, the samples were ultrasonically washed by acetone for 10 minutes and then heated up to 200 °C. Magnetic field resources (arc filter) adjusted at 45 ° positions were employed to remove macro size particles. The process was performed by a cathodic arc PVD system supplied by Ti(Si)Al and CrAl cathodes (Φ140×12 mm3and 99.9% purity) for the deposition of Ti-Al-Cr-C-N and Ti-Al-Cr-Si-C-N films. At first, ion sputtering was done by ionized Ar flow with 10-3 mbar pressure for 60 min at 2.5 KV-DC sample bias, which resulted in surface cleaning and the substrate temperature increase. Then, the chamber gas mixture was changed to (Ar)0.3(N2)0.7 with 10-3 mbar pressure and Ti0.4Al0.6 target and after 5 min Cr0.3Al0.7 target were activated at 150 A current and 40 V bias for 5 min, leading to the coating of the substrate surface by Ti-Al-N and Al-Cr-N films , respectively (Fig. 1). Afterwards, (Ar)0.1(CH4)0.45(N2)0.45 gas mixture was selected for the chamber and both Ti0.4Al0.6 and Cr0.3Al0.7 cathodes were simultaneously activated for 50 min at a similar bias and current, leading to the coating of the Ti-Al-Cr-C-N film (main film) and hence the production of the TiAlCrCN sample. The Ti-Al-N and Al-Cr-N films were deposited before the main film for the achievement of enough adhesion (strong bonding) between the substrate and the Ti-Al-Cr-C-N film. Similar to the TiAlCrCN sample, the TiAlCrSiCN one was produced under the same

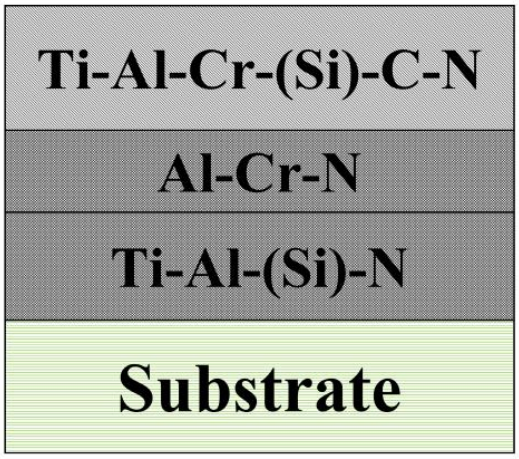

Fig. 1. Different films coated on the used substrate.

conditions but only Ti0.4Si0.1Al0.5 cathode was used instead of Ti0.4Al0.6, leading to the deposition of Ti-Al-Si-N, Al-Cr-N, and Ti-Al-Cr-Si-C-N films, respectively.

2-2- Microstructural characterization

An optical PME3 microscope (OM) and a ZEISS field emission scanning electron microscope (FESEM) equipped with EDS device were employed for microstructure characterization, which involved determination of chemical composition, thickness and growth morphology of the coated films as well as surface morphology. X-ray diffractometry (MPD-X´PERT) was carried out using Cu-Kα radiation with 1.542314A° wave length at a 30 to 70° scan range, 0.03° step size and 1 sec scan step time for phasic characterization.

2.3. Properties evaluation

A stylus profilometer with 5 μm tip radius and an atomic force microscope (AFM) used in 30 nN contact force, 24 μm/s scan velocity and 10 nm curvature tip radius under ambient conditions were employed for the determination of surface topography. Hardness (H) and reduced modulus (E) related to the films were obtained by a nano-indenter with Berkovich-type diamond indenter tip and a loading range from 0.1 to 30 mN at load–unload mode investigated by the Oliver and Pharr method [14]. In addition, surface hardness of the coated samples (film + substrate) was measured using a Vickers micro-hardness tester at 200 gf load. Tribological properties were investigated using a pin-on-disk tribometer equipped with Al2O3 spherical pins with 5 mm diameter and 20 nm surface roughness (Ra) at 0.1 m/s specimen rotation, 20 N normal load, ambient temperature, 25 % relative humidity and 200 m un-lubricated sliding distance, according to the ASTM G7705 standard [15].

3- Results and discussion

3-1- Microstructure

Fig. 2 exhibits FESEM micrographs of the cross-sectional morphology of the coated zone in the TiAlCrCN and TiAlCrSiCN samples. As can be seen, the TiAlCrCN sample has about 2400 nm coated zone thickness, consisting of 1200, 400 and 800 nm for Ti-Al-Cr-C-N, Cr-Al-N and Ti-Al-N films, respectively. On the other hand, in the TiAlCrSiCN kind, Ti-Al-Cr-Si-C-N, Cr-Al-N and Ti-Al-Si-N films have about 1300, 400 and 1000 nm thicknesses, respectively and 2700 nm total thickness. Therefore, the presence of Si has led to the increase of the film thickness, in agreement with Refs [16-17]. The thickness of all films is relatively uniform at different points. Growth morphology and its rate is another noticeable issue in the micrographs as Ti-Al-Si-N and Ti-Al-N films have respectively 200 and 160 nm/min growth rate with a columnar and coarse morphology observed in some previous works [16-19], compared to the other films with un-columnar status and lower growth rate. This is due to the absence of arc filter in the deposition of the Ti-Al-Si-N and the Ti-Al-N kinds, resulting in the deposition of both micro and macro-size particles in addition to nano particles and thus a coarse film, dissimilar to the other films with utilization of arc filter leading to only

micro-size and nano size deposited particles and hence a fine film with lower growth rate (the Ti-Al-Cr-C-N, Ti-Al-Cr-Si-C-N and Cr-Al-N kinds have 24, 26 and 80 nm/min growth rate). As can be seen, Si-incorporated films have a further growth rate than the Si-emptied equal films. The Cr-Al-N kind has a similar thickness, morphology, and growth rate in both samples.

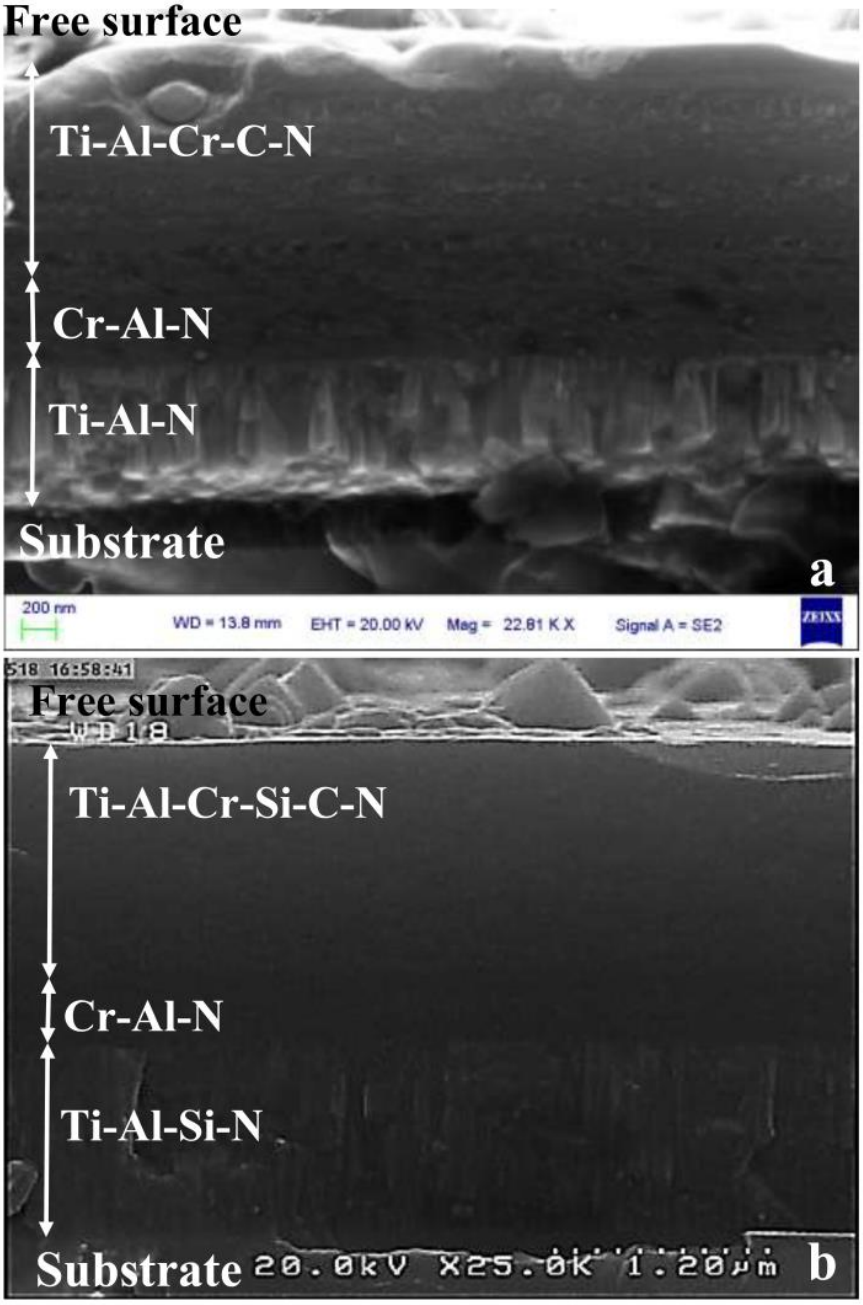

Fig. 2. FESEM images of the coated zone in the TiAlCrCN (a) and TiAlCrSiCN (b) samples.

3-2- Surface morphology

AFM images of the free surface related to the different films have been shown in Figs. 3 and 4. As can be seen, the PVD-coated surfaces of the TiAlCrCN and TiAlCrSiCN samples exhibit some crater-shaped shallow depressions and spherical droplets (growth defects), a prevalent phenomenon in the PVD-coated samples and its origin is large droplets (big particles) deposited on the sample surface during the process [20-22].

The surface of the Ti-Al-Cr-C-N film exhibits about 100 nm maximum depth of the depressions and 1500 nm maximum height of the droplets and the weak bonding leads to the removal of some of these droplets and thus surface depressions are created. The surface of the Ti-Al-Cr-C-N film has about 160 nm average roughness (RMS) with a consideration of growth defects (unreal value) and 9.7 nm roughness without growth defects (actual value). While smaller droplets and more-shallow depressions are distributed on the Ti-Al-Cr-Si-C-N film, meaning a lower roughness (130 nm as unreal roughness and 4.6 nm as its actual value) than that of the Ti-Al-Cr-C-N one. Therefore, incorporation of Si has led to a smoother surface, in agreement with several previous works as [16] which reported that the presence of the Si element inside the film leads to lower surface roughness.

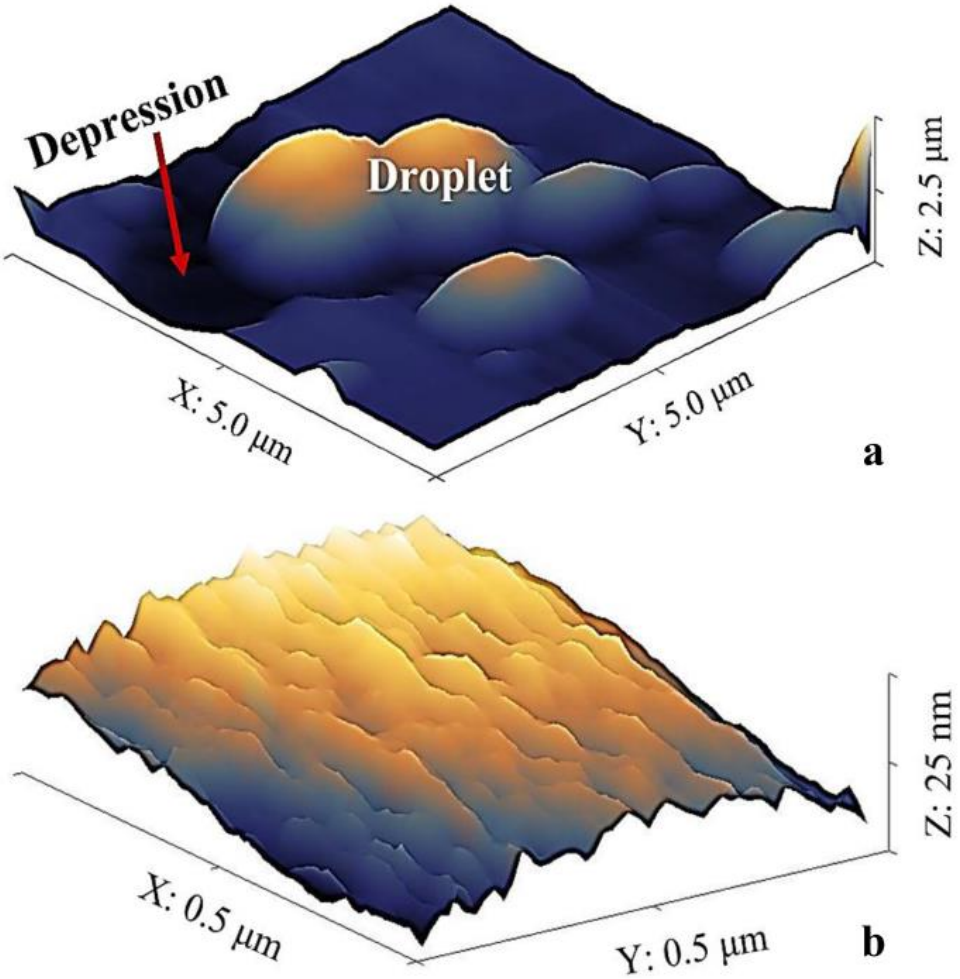

Fig. 3. AFM images of the external surface of the Ti-Al-Cr-Si-C-N film a) with growth defects and b) without defects.

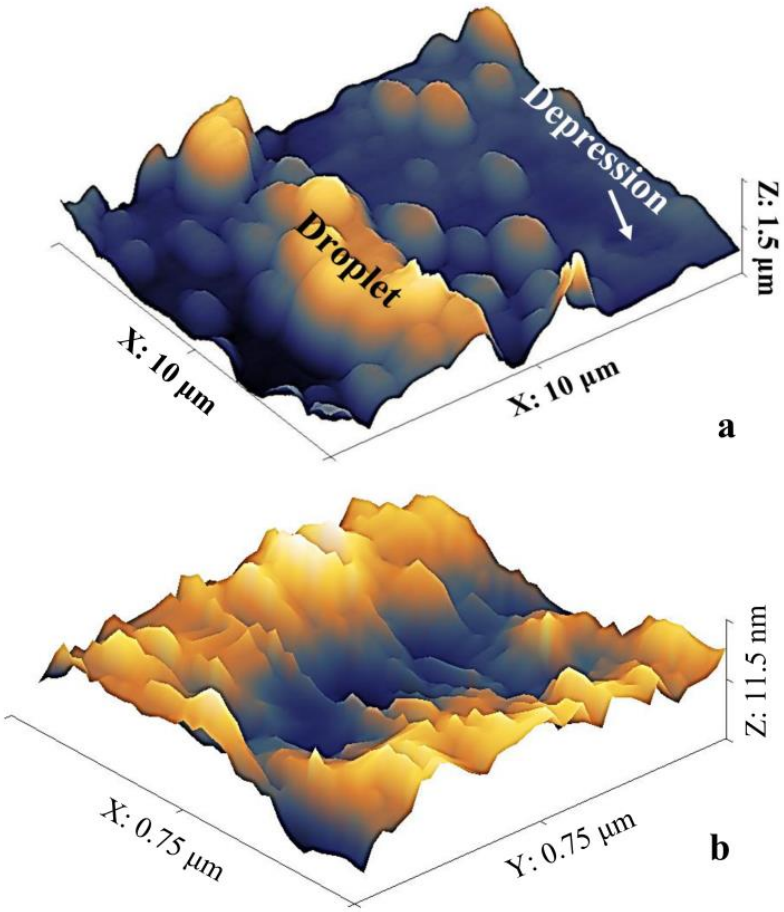

Fig. 4. AFM images of the external surface of the Ti-Al-Cr-C-N film a) with growth defects and b) without defects.

It is predicted that the TiAlCrSiCN sample has a lower friction coefficient and thus better tribological properties than the TiAlCrCN one. Fig.5 shows an FESEM image of the external surface of the PVD-coated sample in the present work. As it is shown, droplets and depressions are distributed on the whole surface.

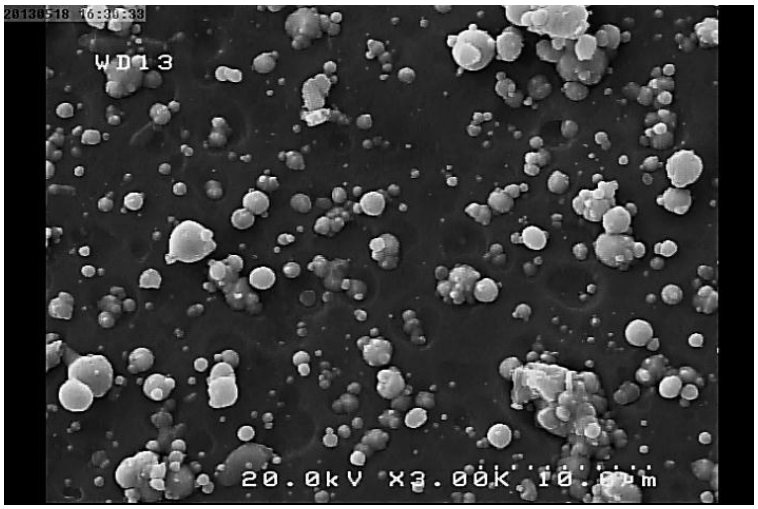

Fig. 5. FESEM image of the external surface of the coated sample showing droplets and depressions.

3-3- X-ray diffractometry

EDS patterns related to the TiAlCr(Si)CN films have been shown in Figs. 6 and 7. As it is shown, Ti, Al, Cr, C and N elements are available in both of the as-deposited films, while Si has been inserted into the TiAlCrSiCN one; with Ti0.58Al0.26Cr0.07C0.04N0.03 and Ti0.59Al0.22Cr0.07Si0.02C0.04N0.03 chemical composition, respectively. Irrespective of Si, Ti has the maximum percent and N minimum value in both analyses.

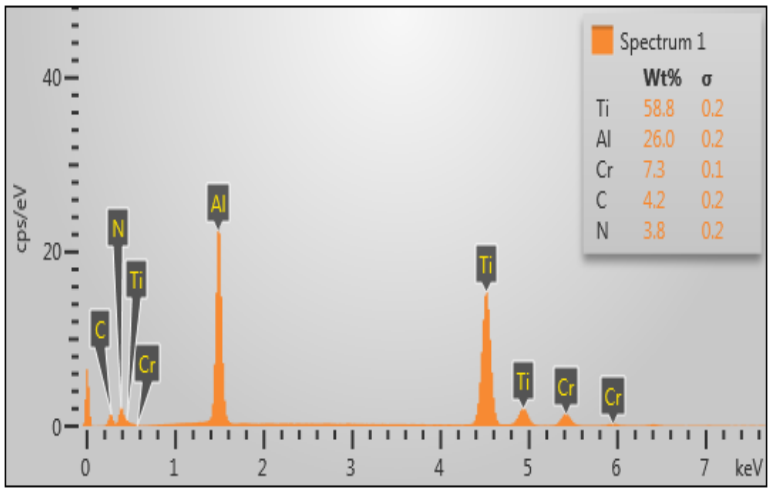

Fig. 6. EDS analysis of the Ti-Al-Cr-C-N film.

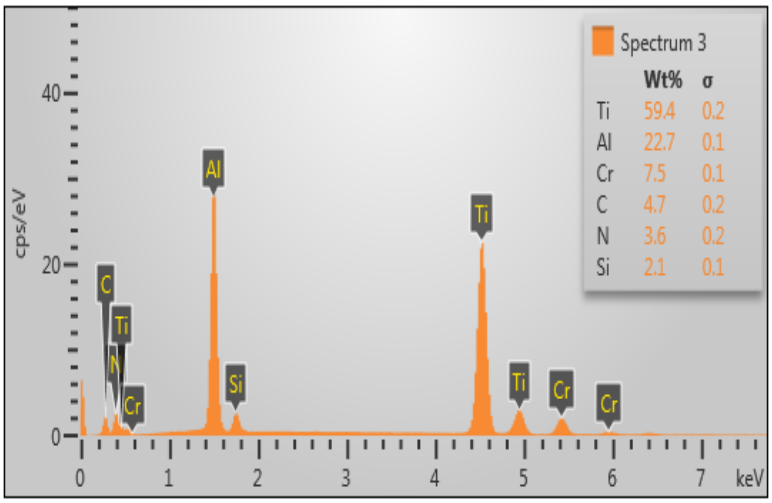

Fig. 7. EDS analysis of the Ti-Al-Cr-Si-C-N film.

Fig. 8 shows X-ray diffraction patterns for the coated samples. Due to the low thickness of the coated zone, its peaks have a low intensity in comparison to the substrate. The peaks of both films exhibit a FCC-structured single phase corresponding to (111), (200), (220) and (311) planes, in agreement with [19, 23, 24]. The XRD spectrum of the Ti-Al-Cr-Si-C-N film does not show any crystallite Si-incorporated phase (e.g. CrSi, TiSi and Si3N4) indicating that Si may be available in an amorphous state, according to several researches [25-28]. For example, Guangan et al. [25] exhibited the presence of the amorphous Si3N4 phase in Cr-Si-N film by FITR and XPS analyses. On the other hand, the Ti-Al-Cr-Si-C-N film may be a mixed film in which the TiAlCr(C,N) crystallites are distributed in the Si(C,N) amorphous matrix [29-32]. The Ti-Al-Cr-C-N and Ti-Al-Cr-Si-C-N films have respectively crystallite sizes about 11.7 and

9.5 nm measured by the Scherer equation [33], agreeing with Ref [16] which demonstrated that the addition of Si into the deposited film led to lower grain size. As it is shown, the existence of Si has resulted in 2θ reduction, FWHM increase and hence reduction of the grain size that may be due to the increase of internal stress sites by Si content, as shown in other Refs [34, 35]. The card numbers [00-037-1140] and [00-029-0017] were utilized in the X-ray diffraction.

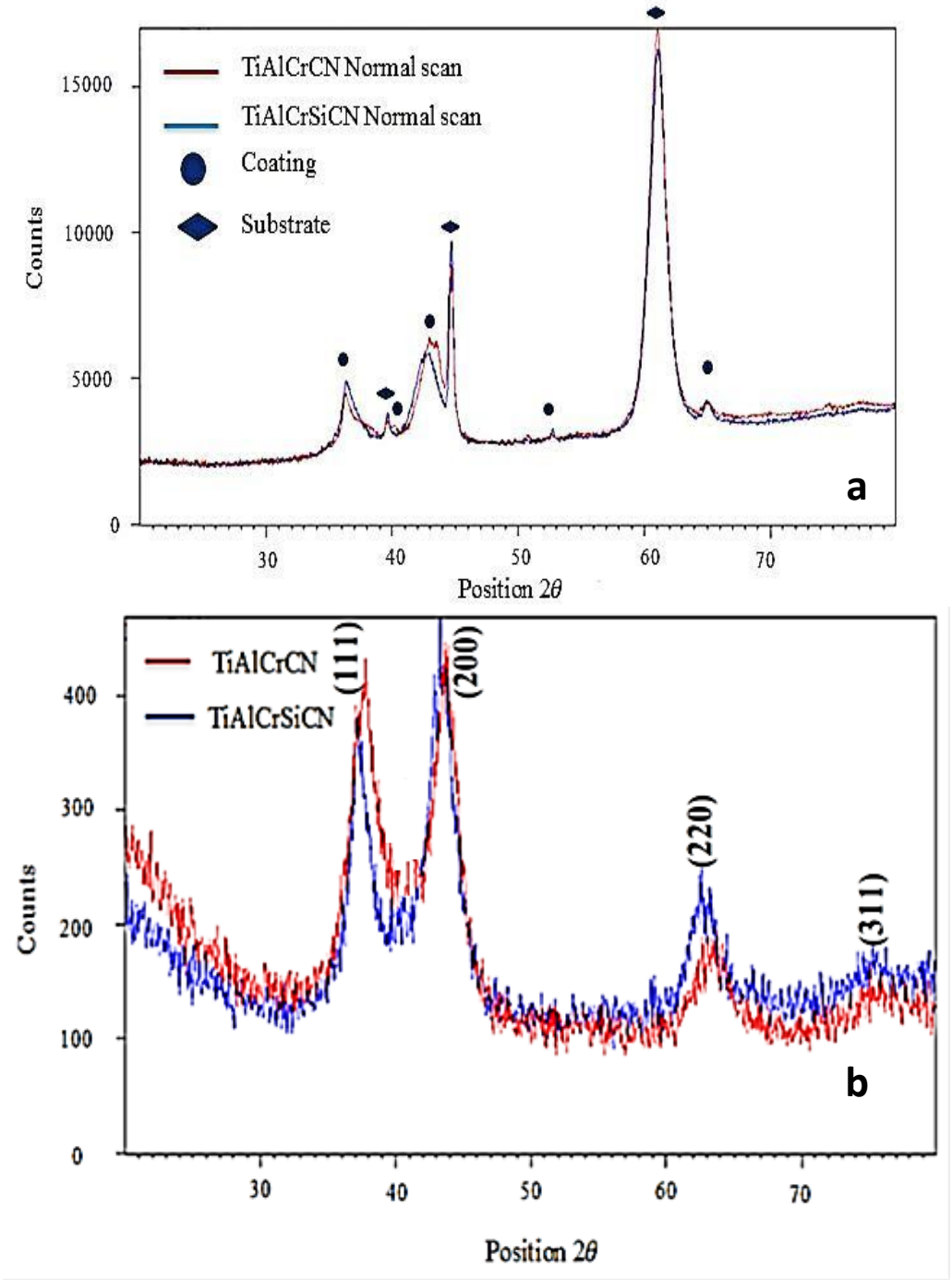

Fig. 8. X-ray patterns under different process conditions, a) the coated samples, b) only coated films.

3-4- Hardness, reduced modulus and H/E ratio

Surface hardness (H), reduced modulus (E) and H/E values obtained by nano-indentation testing on the coated surfaces using load-unload mode and some other properties are listed in Table 2. Both of the coated films exhibit a higher hardness than the tool steel substrate, leading to an increase in surface hardness of the coated tool steel . The Ti-Al-Cr-Si-C-N film presents the highest values of hardness, reduced modulus and H/E ratio compared with the other film, revealing that Si has an effective role in enhancing the steel properties. In the absence of of the Si element, only solid solution hardening mechanism inhibits mobility of dislocations, resulting in hardness enhancement [22].While the Si component leads to the formation of Si(C,N) amorphous phase as Si3N4 and SiC combined with the TiAlCr(C,N) solid solutions crystallites distributed in the Si(C,N) amorphous matrix (according to the XRD results), leading to the achievement of a nano-structured film composed of an amorphous matrix and solid solution crystallites in which the inhibition of dislocations on the location of "crystallite– amorphous phase" boundary leads to the hardness enhancement, in agreement with Refs [16, 26, 29] which demonstrated that a higher hardness is achieved by the Si presence. In addition, micro-hardness test on the substrate and both the TiAlCrCN and TiAlCrSiCN specimens was carried out at 200 gf force, yielding 2.16, 8.7 and 10.8 GPa as the hardness values, respectively. Because of the relatively high value of the selected force, the obtained hardness is related to both the coated zone and near-surface regions of the substrate. Therefore, the SPK 1.2080 tool steel with higher surface hardness is achieved by the deposition of the Si-incorporated Ti-Al-Cr-C-N coating.

Table 2. Some properties of the Si-incorporated and Si-emptied films.

Film	Thickness (μm)	Crystallite grain size (nm)	Surface roughness		E (GPa)	H (GPa)	H/E
			Sa1 (nm)	Sa2 (nm)			
TiAlCrCN	2.4±0.2	11.7	160±20	9.7±0.2	364±25	27.5±0.5	0.075
TiAlCrSiCN	2.7±0.2	9.5	130±15	4.6±0.13	477±28	38.5±0.5	0.081

(RMS) Sa1= consideration growth defects, Sa2=without growth defects

3-5- Tribological properties

Friction coefficient curves related to the SPK 1.2080 tool steel under different treatment conditions have been illustrated in Fig. 9. According to this figure, the deposition of the Ti-Al-Cr-C-N and Ti-Al-Cr-Si-C-N films has produced a lower friction coefficient, 0.45 and 0.35 values in the TiAlCrCN and TiAlCrSiCN specimens, respectively. There are some peaks at the TiAlCrCN and TiAlCrSiCN plots, indicating abrasion wear affected by spherical droplets with weak bonding that are removed from the film surface by slider pin during wear testing, in agreement with Ref [36] where low-bonded surface droplets were removed from the surface by wear testing and led to an accelerated wear. The average value of friction coefficient for the TiAlCrSiCN sample is lower than that of the TiAlCrCN one, due to the smaller droplets and more-shallow depressions in the Si-incorporated film with 4.6 nm roughness compare to the Si-emptied film with 9.7 nm roughness.

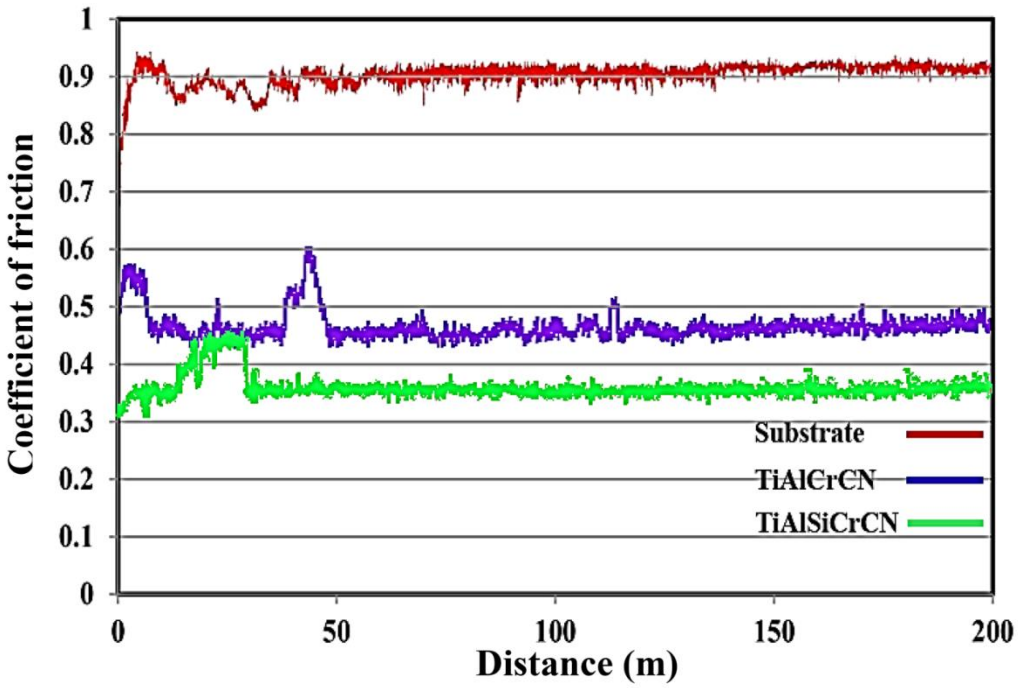

Fig. 9. Friction coefficient curves of the tool steel under different process conditions.

4-Conclusions

- Ti-Al-Cr-(Si)-C-N nanocomposite films were coated on the SPK 1.2080 tool steel substrate.
- The coated films had about 2.5 μm uniform thickness and a nano-size structure and the existence of Si was led to a thicker film containing crystallites with smaller sizes.
- Surface hardness of the steel increased by a factor of about 14 and 18 by deposition of the Ti-Al-Cr-C-N and Ti-Al-Cr-Si-C-N films, respectively.
- The friction coefficient was significantly reduced by the Si-emptied and Si-incorporated films.
- The Si-incorporated Ti-Al-Cr-C-N film led to better properties, namely, further thickness, hardness, reduced modulus and H/E ratio as well as lower roughness and friction coefficient in the SPK 1.2080 cold-work tool steel.

References

[1]. S. Hofmann, Formation and diffusion properties of oxide films on metals and on nitride coatings studied with auger electron spectroscopy and X-ray photoelectron spectroscopy, Th. Sol. Fil. Vol.193–194, 1990, pp. 648-664.

[2]. T. Matsue, T. Hana Busa, Y. Ikeuchi, Dependence to processing conditions of structure in TiN films deposited by arc ion plating, Vac., Vol. 74, 2004, pp. 647-51.

[3]. D.K. Lee, D.Sh. Kang, J. Hyung Suh, Ch.G. Park, K.H. Kim, Synthesis and mechanical evaluation of quaternary Ti–Cr–Si–N coatings deposited by a hybrid method of arc ion plating and sputtering techniques, Sur. Coat. Tech., Vol. 200, 2005, pp. 1489-94.

[4]. P.L. Tam, Z.F. Zhou, P.W. Shum and K.Y. Li, Structural, mechanical, and tribological studies of Cr–Ti–Al–N coating with different chemical compositions, Th. Sol. Film., Vol. 516, 2008, pp. 5725–5731.

[5]. Y.Y. Chang, C.P. Chang, D.Y. Wang, S.M. Yang and W. Wu, High temperature oxidation resistance of CrAlSiN coatings synthesized by a cathodic arc deposition process, J. All. Com., Vol. 46, 2008, pp. 336-341.

[6]. J.J. Nainaparampil, J.S. Zabinski and A. Korenyi, Formation and characterization of multiphase film properties of (Ti–Cr) N formed by cathodic arc deposition, Th. Sol. Fil., Vol. 333, 1998, 88-94.

[7]. J.H. Park, W.S. Chung, Y.R. Cho and K.H. Kim, Synthesis and mechanical properties of Ti–Si–N coatings deposited by a hybrid system of arc ion plating and sputtering techniques, Sur. Coat. Tech., Vol. 188–189, 2004, pp. 425-430.

[8]. C.W. Zou, J. Zhang, W. Xie, L.X. Shao, D. Li, D.J. Fu, Synthesis and mechanical properties of quaternary Ti–Cr–Si–N nanocomposite coatings deposited by closed field unbalanced middle frequency magnetron sputtering, J. All. Com., Vol. 529, 2012, pp. 52–57.

[9]. S. PalDey, S.C. Deevi, Single layer and multilayer wear resistant coatings of (Ti,Al)N: a review, Mater. Sci. and Eng., Vol. A 342, 2003, pp. 58–79.

[10]. L.F. Senn, C.A. Achete, T. Hirsch, F.L. Freire, Structural, chemical, mechanical and corrosion resistance characterization of TiCN coatings prepared by magnetron sputtering, Sur. Coat. Tech., Vol. 94–95, 1997, pp. 390–397.

[11]. Q. Wang, F. Zhou, X. Wang, K. Chen, M. Wang, T. Qian and Y. Li, Comparison of tribological properties of CrN, TiCN and TiAlN coatings sliding against SiC balls in water, Appl. Sur. Sci., Vol. 257, 2011, pp. 7813–7820.

[12]. E.W. Niu, L.Li, G.H. Lv, H. Chen, X.Z. Li, X.Z. Yang, S.Z. Yang, Characterization of Ti–Zr–N films deposited by cathodic vacuum arc with different substrate bias, Appl. Sur. Sci., Vol. 254, 2008, pp. 3909–3914.

[13]. J. Shi, C.M. Muders, A. Kumarb, X. Jiang, Z.L. Pei, J. Gong and C. Sun, Study on nanocomposite Ti–Al–Si–Cu–N films with various Si contents deposited by cathodic vacuum arc ion plating, Appl. Sur. Sci., Vol. 258, 2012, pp. 9642– 9649.

[14]. W.C. Oliver, G.M. Pharr, Measurement of hardness and elastic modulus by instrumented indentation: advances in understanding and refinements to methodology, J. Mater. Res., Vol. 19, 2004, pp. 3-20.

[15]. ASTM G77-05, Standard test method for ranking resistance of materials to sliding wear using block-on-ring wear test, USA ASTM International 2005.

[16]. H.W. Strauss, R.R. Chromik, S.Hassan and J.E. Klemberg-Sapieha, In situ tribology of nanocomposite Ti–Si–C–H coatings prepared by PE-CVD, Wea., Vol. 272, 2011, pp. 133–148.

[17]. Li. Chen, K.K. Chang, D. Yong, J.R. Li and M.J. Wu, A comparative research on magnetron sputtering and arc evaporation deposition ofTi–Al–N coatings, Th. Sol. Fil., Vol. 519, 2011, pp. 3762–67.

[18]. C.H. Hsu, C.K. Lin, K.H. Huang, K.L. Ou, Improvement on hardness and corrosion resistance of ferritic stainless steel via PVD-(Ti,Cr)N coatings, Sur. Coat. Tech., Vol. xxx, 2012, pp. xxx–xxx.

[19]. Li. Chen, K.K. Chang, D. Yong, J.R. Li and M.J. Wu, A comparative research on magnetron sputtering and arc evaporation deposition of Ti–Al–N coatings, Thi. Sol. Film., Vol. 519, 2011, pp. 3762–67.

[20]. W. Rong hua, Plasma enhanced magnetron sputter deposition of Ti-Si-C-N based nanocomposite coatings, Sur. Coat. Tech., Vol. 203, 2008, pp. 538-544.

[21]. C. Martini, L.Ceschini, A comparative study of the tribological behavior of PVD coatings on the Ti-6Al-4V alloy, Tri. Inter., Vol. 44, 2011, pp. 297–308.

[22]. Li. Qiang, J. Fan-qing, L. Yong-xiang, W. Rong-hua, N. Huang, Microstructure and tribological properties of Ti(Cr)SiCN coating deposited by plasma enhanced magnetron sputtering, Vac., Vol. 89, 2013, pp. 168-173.

[23]. H. Willmann, P.H. Mayrhofer, P.O. Persson, A.E. Reiter, L. Hultman and C. Mitterer, Thermal stability of Al–Cr–N hard coatings,Scr. Mater., Vol. 54, 2006, pp. 1847-51.

[24]. A. Kimura, M. Kawate, H. Hasegawa and T. Suzuki, Anisotropic lattice expansion and shrinkage of hexagonal TiAlN and CrAlN films,Sur. Coat. Tech., Vol. 169, 2003, pp. 367.

[25]. Zh. Guangan, W. Liping, W. SC, Y. Pengxun and X. Qunji, Structure and mechanical properties of reactive sputtering CrSiN films, Appl. Sur. Sci., Vol. 255, 2009, pp. 4425-29.

[26]. D. Mercs, P. Briois andV. Demange, Influence of the addition of silicon on the structure and properties of chromium nitride coatings deposited by reactive magnetron sputtering assisted by RF plasmas, Sur. Coat. Tech., Vol. 201, 2007, pp. 6970-76.

[27]. M. Nose, Y. Deguchi, T. Mae, E. Honbo, T. Nagae andK. Nogi, Influence of sputtering conditions on the structure and properties of Ti-Si-N thin films prepared by r.f.-reactive sputtering, Sur. Coat. Tech., Vol.174-175, 2003, pp. 261-65.

[28]. D. Pilloud, J.F. Pierson, A.P. Marques and A. Cavaleiro, Structural changes in Zr-Si-N films vs. their silicon content, Sur. Coat. Tech., Vol. 180-181, 2004, pp. 352-56.

[29]. Z.w. Xie, L.p. Wang, X.f. Wang, L. Huang, Y. Luand J.c. Yan, Influence of Si content on structure and mechanical properties of TiAlSiN coatings deposited by multi-plasma immersion ion implantation and deposition, Tran. Nonf. Met. Soc. Chi., Vol. 21, 2011, pp. 476-482**.**

[30]. S. Vepřek, S.G. Prilliman and S.M. Clark, Elastic moduli of nc-TiN/a-Si3N4 nanocomposites: Compressible, yet superhard, J.Ph. Chem. Sol., Vol. 71, 2010, pp. 1175-78**.**

[31]. S. Veprek, S. Reiprich and L. Shizhi, Superhard nanocrystalline composite materials: The TiN/Si< inf>3</inf> N< inf> 4</inf> system,Appl.Phy.Lett., Vol. 66, 1995, pp. 2640-42**.**

[32]. K. Yamamoto, S. Kujime, K. Takahara, Structural and mechanical property of Si incorporated (Ti,Cr,Al)N coatings deposited by arc ion plating process, Sur. Coat. Tech., Vol. 200, 2005, pp. 1383–1390.

[33]. A.L. Patterson, The Scherer formula for X-ray particle size determination, Phys. Revie., Vol. 56, 1939, pp. 978–982.

[34]. S. Carvalho, E. Ribeiro, L. Rebouta, C. Tavares, J. P. Mendonça, A. Caetano Monteiro, et al., Microstructure, mechanical properties and cutting performance of superhard (Ti,Si,Al)N nanocomposite films grown by d.c. reactive magnetron sputtering, Sur. Coat. Tech., Vol. 177–178, 2004, pp. 459-468.

[35]. A. Flink, J. M. Andersson, B. Alling, R. Daniel, J. Sjölén, L. Karlsson, et al., Structure and thermal stability of arc evaporated (Ti0.33Al0.67); xSixN thin films, Thi. Sol. Film., Vol. 517, 2008, pp. 714-721.

[36]. X.z. Ding, C.T. Bui and X.T. Zeng, Abrasive wear resistance of TiAlN hard coatings deposited bya vacuum arc system with lateral rotating cathodes, Sur.Coat. Tech., Vol. 203, 2008, pp. 680-684**.**